

Mixing processes during the evolution of red giants with moderate metal deficiencies : the role of molecular-weight barriers^{*}

Corinne Charbonnel^{1,2}, Jeffery A. Brown^{3,4}, George Wallerstein^{3,5}

¹ Laboratoire d'Astrophysique de Toulouse, CNRS UMR 5572, Toulouse, France

² Space Telescope Science Institute, 3700 San Martin Drive, Baltimore, MD 21218, USA

³ Dept. of Astronomy, University of Washington, Box 351580, Seattle, WA 98195-1580, USA

⁴ Program in Astronomy, Washington State University, Pullman, WA 99164-3113, USA

⁵ Guest observer, Dominion Astrophysical Observatory, Herzberg Institute of Astrophysics, National Research Council, Canada
Corinne.Charbonnel@obs-mip.fr, jbrown@delta.math.wsu.edu, wall@astro.washington.edu

May 12, 2018

Abstract. We have assembled accurate abundance data for Li, C, and N as well as the $^{12}\text{C}/^{13}\text{C}$ ratio for five field giants with $[\text{Fe}/\text{H}] \simeq -0.6$ including Arcturus and two stars in the globular cluster 47 Tuc. Using their very precise M_{bol} values obtained from HIPPARCOS parallaxes, we can place them into an evolutionary sequence. The sequence shows that the $^{12}\text{C}/^{13}\text{C}$ ratios drops from ~ 20 to near 7 between $M_{\text{bol}} = +1$ and $+0.5$, while Li disappears. At the same time the $^{12}\text{C}/^{14}\text{N}$ ratio diminishes by 0.2 to 0.4 dex. The two stars in 47 Tuc with M_{bol} near -2.0 show even lower $^{12}\text{C}/^{14}\text{N}$ ratios by 0.4 dex indicating further mixing as they evolved to the top of the red giant branch.

These observations confirm the existence of an extra-mixing process that becomes efficient on the red giant branch only when the low-mass stars reach the so-called luminosity function bump. We use the values of the carbon isotopic ratio observed in our sample to get constraints on the μ -barriers that may shield the central regions of a star from extra-mixing. We show that the same value of the critical gradient of molecular weight leads to $^{12}\text{C}/^{13}\text{C}$ ratios observed at different metallicities. This “observational critical μ -gradient” is in very good agreement with the one which is expected to stabilize meridional circulation. This result provides strong clues on the nature of the extra-mixing which occurs on the RGB, and indicates that it is related to rotation.

Key words: stars: abundances – stars : evolution - stars : interiors - stars : giant

Send offprint requests to: Corinne Charbonnel

^{*} Based partially on observations obtained at the Dominion Astrophysical Observatory, National Research Council, Canada

1. Introduction

For some time now it has been clear that evolved low mass stars exhibit chemical anomalies which are not predicted by standard stellar evolution theory. By “standard” we refer to the hypotheses that stellar convective regions are instantly mixed and that no transport of chemicals occurs in the radiative regions. In addition, standard models are those without rotation at any depth. With these assumptions, changes in the surface abundances prior to the asymptotic giant branch (AGB) stage are only expected to be due to convective dilution during the first dredge-up phase. In low mass red giant branch (RGB) stars, the convective envelope reaches only regions where ^{12}C was processed to ^{13}C and ^{14}N . Consequently, the carbon isotopic ratio declines (from 90 to about 20-30), the carbon abundance drops (by about 30%) and nitrogen increases (by about 80%), but oxygen and all heavier element abundances remain unchanged. According to the standard scenario, the surface abundances then stay unaltered as the convective envelope slowly withdraws outward in mass during the end of the RGB evolution.

However, observational data reveal a different reality. The first discrepancy came among the first stellar $^{12}\text{C}/^{13}\text{C}$ ratios published (Day et al. 1973), when Arcturus was found to have $^{12}\text{C}/^{13}\text{C} = 7.2 \pm 1.5$. The discrepancy was aggravated by the analysis by Lambert & Ries (1981) of C, N, and O abundances in a sample of red giants, including Arcturus. In fact, in most of the metal-deficient field and globular cluster evolved stars, the observed conversion of ^{12}C to ^{13}C and ^{14}N greatly exceeds the levels expected from standard stellar models; the $^{12}\text{C}/^{13}\text{C}$

ratio even reaches the near-equilibrium value in many Pop II RGB stars (Snedden, Pilachowski & Vandenberg 1986; Smith & Suntzeff 1989; Brown & Wallerstein 1989, 1992; Gilroy & Brown 1991, henceforth GB91; Brown, et al.1990, henceforth BWO; Bell et al. 1990; Suntzeff & Smith 1991; Shetrone et al. 1993, henceforth SSP93; Briley et al. 1994, 1997). This problem actually also occurs, but to a somewhat lower extent, in evolved stars belonging to open clusters with turnoff masses lower than $2M_{\odot}$ (Gilroy 1989; GB91).

In addition, Population II evolved stars present other chemical anomalies. In halo giants, the lithium abundance continues to decrease after the completion of the first dredge-up (Pilachowski et al. 1993). A continuous decline in carbon abundance with increasing stellar luminosity along the RGB is observed in globular clusters such as M92 (Carbon 1982; Langer et al.1986), M3 and M13 (Suntzeff 1981), M15 (Trefzger et al.1983), NGC 6397 (Bell et al.1979, Briley et al.1990), NGC 6752 and M4 (Suntzeff & Smith 1991). In some globular clusters (M92, Pilachowski 1988; M15, Sneden et al.1991; M13, Brown et al.1991, Kraft et al.1992; ω Cen, Paltoglou & Norris 1989), giants exhibit evidence in their atmospheres for O \rightarrow N processed material. In addition to the O versus N anticorrelation, the existence of Na and Al versus N correlations and Na and Al versus O anticorrelations in a large number of globular cluster red giants has been clearly confirmed (Drake et al.1992, Kraft et al.1992, 1993, Norris & Da Costa 1995, Kraft 1994, Kraft et al.1997, Shetrone 1996, Zucker et al.1996).

These observations suggest that low mass stars undergo a non-standard mixing process which adds to the first dredge-up and modifies the surface abundances. The first and only evidence on the evolutionary state at which this non-standard mixing actually becomes effective came from observations of the C/N and $^{12}\text{C}/^{13}\text{C}$ ratios (respectively by Brown 1987 and by GB91) in evolved stars of M67. In this old open cluster, which has a turnoff mass of $1.2 M_{\odot}$ (VandenBerg 1985, Meynet et al.1993) and a value of $[\text{Fe}/\text{H}]=0.0\pm 0.1$, the observational and theoretical first dredge-up appear to be in complete agreement (Charbonnel 1994, henceforth C94). Indeed, the $^{12}\text{C}/^{13}\text{C}$ ratio changes at the base of the giant branch from a value >40 to 21-25 between $M_{\text{v}} \approx +3.5$ and $M_{\text{v}} \approx +2.5$; C/N changes by about a factor of 4 in this same interval. The onset of the dredge-up occurs at a luminosity in accord with standard theory, and the observed post-dilution ratios are in very good agreement with the standard predictions at this point. However, in M67 an additional mixing event begins at about $M_{\text{v}} \approx +0.5$ where $^{12}\text{C}/^{13}\text{C}$ drops from 21-25 to 11-15. This luminosity actually corresponds to the so-called ‘‘bump’’ in the RGB luminosity function (Fusi-Pecci et al.1990), i.e., to the evolutionary point where the hydrogen burning shell crosses the chemical discontinuity created by the convective envelope at its maximum extent. As pointed out by C94, this observational fact

strongly suggests that prior to this evolutionary point the mean molecular weight gradient created during the first dredge-up acts as a barrier to any mixing below the convective envelope. After this point, however, the gradient of molecular weight above the hydrogen-burning shell is much lower, and extra-mixing is free to act.

Since the observations in M67, there have been no new sets of abundance data in any cluster, either globular or galactic, to establish the evolutionary point at which the extra-mixing begins to occur. With 4-meter class telescopes it is almost impossible to observe red giants in globular clusters at the luminosities at which $^{12}\text{C}/^{13}\text{C}$ is expected to drop from near 20 to less than 10 because the molecular bands become weaker with increasing temperature and gravity. Furthermore, the attainable signal-to-noise of the spectra diminishes with decreasing stellar luminosity. It is crucial, however, for our understanding of the nature of the process to compare conditions in stars of different populations and metallicities.

To this end, we address here the problem of the onset of the extra-mixing, and of its possible metallicity dependence, by placing in an evolutionary sequence five field giants with moderate metal deficiencies and two giants of the globular cluster 47 Tuc for which we have assembled accurate abundance data for Li, C and N as well as for the $^{12}\text{C}/^{13}\text{C}$ ratio. Our observational data are presented in §2. We enlarge our sample by including in our discussion the old disk giants with $^{12}\text{C}/^{13}\text{C}$ ratios derived by SSP93. Very precise absolute magnitudes were recomputed from HIPPARCOS parallaxes for all the stars we consider. As discussed in §3, the sequence allows us to confirm that the discrepancy between observations of mixing-sensitive species and standard theory really appears at the luminosity-function bump (LFB) on the RGB, but not at lower luminosities. Since our sample is moderately metal-deficient, we can study the metallicity-dependence of the extra-mixing by comparing our results with the observations in M67. In §4, we investigate the nature of the factor that stabilizes the star against extra-mixing before it reaches the luminosity-function bump, and discuss the role of molecular-weight (μ) barriers. From simple considerations, we derive from our data the ‘‘observational’’ critical μ -gradient, $(\nabla \ln \mu)_{c,obs}$, that shields the central regions of a star from extra-mixing. If we assume that extra-mixing is free to act down to the layers defined by the same value of $(\nabla \ln \mu)_{c,obs}$ whatever the stellar mass and metallicity, then $^{12}\text{C}/^{13}\text{C}$ ratios can be explained both for Pop I and II giants. Finally, we discuss the implications for the nature of the extra-mixing mechanism itself on the RGB, and bring clues that it may be related to rotation-induced processes.

2. Observational data for metal poor stars

Some of the data that we employ here have already been published. We concentrate on stars of modest metal defi-

Table 1. Observed Stars ^a

HD	Star	V - K	T _{eff}	M _V	M _{bol}	log g	[Fe/H]
37160	ϕ^2 Ori	2.41	4720	+1.33± 0.07	+0.89	2.45	-0.70
3546	ϵ And	2.13	4925	+0.77± 0.09	+0.43	2.34	-0.66
89484	γ Leo A	—	4440	-0.32±0.07	-0.9	1.62	-0.46
89485	γ Leo B	—	4900	+0.87±0.07	+0.5	2.36	-0.42
124897	Arcturus	3.00	4330	-0.30±0.02	-0.98	1.55	-0.62
—	47 Tuc 3501	3.45	3975	-1.1	-1.9	0.9	-0.65
—	47 Tuc 4418	3.50	3975	-1.1	-1.9	0.9	-0.65

^a The stars were selected so as to be as close to the evolutionary tracks delineated by the color-magnitude diagram of 47 Tuc as their parallaxes (ground based when we selected the stars) and [Fe/H] values from the literature permitted

Table 2. Comparison of our abundances (upper analysis) with those of Cottrell and Sneden (1986) and Shetrone et al.(1993) (lower analysis) of ϵ And and ϕ^2 Ori

Star	T _{eff}	log g	[Fe/H]	[C/Fe]	[N/Fe]	[O/Fe]	¹² C/ ¹³ C	log ϵ (Li)
ϵ And	4925	2.55	-0.45	-0.29	+0.24	-0.06	7	< -0.2
	4750 ^{a,b}	2.0 ^{a,b}	-0.7 ^{a,b}	-0.15 ^b	-0.10 ^b	+0.2 ^b	7.5 ^a	0.0 ^b
ϕ^2 Ori	4720	2.85	-0.43	-0.03	+0.08	+0.15	>20	+0.3
	4600	2.4	-0.7	0.00	-0.20	+0.15	>40	

^a From Shetrone et al. (1993)

^b From Cottrell and Sneden (1986)

ciency. Five bright metal-deficient field stars are ϕ^2 Ori, ϵ And, γ Leo B, γ Leo A and Arcturus. Their M_{bol} values range from near +0.9 to -1.0 so they form an evolutionary sequence that starts from fainter absolute magnitude than can be reached with high spectral resolution in globular clusters. As a continuation of our “evolutionary sequence” we include two stars from the globular cluster 47 Tucanae whose properties indicate that they are first giant branch (i.e. not AGB) stars. The basic properties of our sample stars are shown in Table 1.

For the field stars we derive the gravity values assuming a mass of 0.8 M_⊙, the HIPPARCOS parallaxes, T_{eff}’s derived from the V - K color-T_{eff} relation (Ridgway et al.1980, DiBenedetto 1993, Dyck et al.1996), and the bolometric corrections of Buser and Kurucz (1992). This method is probably superior to spectroscopic determination of gravities using ionization balance; a test using the HIPPARCOS parallaxes indicates the spectroscopic gravities often are too low by a factor of two (Nissen & Høg 1997). The visual binary stars in γ Leo do not have separate colors; instead, we adjust the spectroscopic T_{eff}’s of Lambert & Ries (1981) downward by 210K, the mean offset between their temperature scale and the V - K scale. We note that the 47 Tuc stars are probably not on the same absolute magnitude scale as the HIPPARCOS results, since they depend upon a cluster distance modulus which probably needs revision in light of the HIPPARCOS

results for the subdwarfs; see, *e.g.*, Reid (1997). For our purposes, the precise value of the absolute magnitudes of the two globular cluster stars is not important: it matters here only that they are ~ 1 mag more luminous than our most luminous field stars. ¹

The abundances we use have been rederived with a number of improvements. For Arcturus and the γ Leo pair we have combined the equivalent widths of Lambert & Ries (1981) and Ries (1981) with the empirical photometric T_{eff} scale and the most recent and almost certainly most accurate value of the CN dissociation potential D_o^o = 7.65 eV (Bauschlicher et al.1988). For 47 Tuc we have used the data of BWO with two changes. The analysis by Hesser et al.(1987) of the color-magnitude diagram of

¹ Both Arcturus and Gamma Leo A lie above the horizontal branch and hence could be post-He-flash stars. However their colors place them on the first ascent giant branch. A comparison of the colors we have quoted shows that Arcturus falls exactly on the first ascent giant branch of 47 Tuc (Hesser et al. 1987). For Gamma Leo the measured B-V color pertains to both stars and must be deconvolved to obtain the color of star A. To derive the observed B-V color of 1.15 mag, we combined the color of Arcturus, B-V=1.23 with that of the G8III secondary, 0.95 mag, using the observed 1.2 visual magnitude difference, to derive the observed composite color of 1.15 mag. This confirms that the color of Gamma Leo A is about the same as that of Arcturus and hence that Gamma Leo A on the first ascent giant branch.

Table 3. Abundance Results

Star	^{12}C	^{13}C	N	O	(C + N) ^a	(C + N + O) ^b	$^{12}\text{C}/^{13}\text{C}$	$\log \epsilon(\text{Li})$
ϕ^2 Ori	7.9	<6.6	7.8	8.55	8.17	8.7	>20 ^c	0.3
ϵ And	7.65	6.8	7.95	8.3	8.15	8.53	7 ^d	< -0.20 ^e
γ Leo B	7.77	6.8	7.87	8.45	8.14	8.62	9.5	$\leq +0.3$ ^f
γ Leo A	7.8	7.0	7.9	8.45	8.18	8.64	6.5	≤ 0.0 ^f
Arcturus	7.9	7.0	7.7	8.55	8.15	8.7	7	< -1.5 ^g
47 Tuc 3501	7.7	6.85	8.25	8.45	8.37	8.7	8	^h
47 Tuc 4418	7.6	6.75	8.25	8.5	8.35	8.7	7	^h
\odot ⁱ	8.6	6.6	8.0	8.9	8.7	9.1	90	1.15

^a This is $^{12}\text{C} + ^{13}\text{C} + \text{N}$

^b This is $^{12}\text{C} + ^{13}\text{C} + \text{N} + \text{O}$

^c Shetrone et al.1993 find $^{12}\text{C}/^{13}\text{C} > 40$

^d Shetrone et al.1993 find $^{12}\text{C}/^{13}\text{C} = 7.5$

^e Shetrone et al.1993 find $\text{Li} = 0.0$

^f Helfer & Wallerstein 1968

^g Lambert et al.1980

^h not present, no upper limit computed

ⁱ photospheric value, Anders & Grevesse 1989, Grevesse et al.1991

47 Tuc indicate an iron abundance for 47 Tuc higher by about 0.2 dex as compared with the BWO value. Hence, we have accepted $[\text{Fe}/\text{H}] = -0.65$ rather than -0.85 for the 47 Tuc stars and have recalculated the CNO abundances using models with the new $[\text{Fe}/\text{H}]$ values. For the $^{12}\text{C}/^{13}\text{C}$ ratio in 47 Tuc star 4418, we have adopted the second solution in Table 2 of Bell et al.(1990; multiple solutions for $^{12}\text{C}/^{13}\text{C}$ and carbon abundance are given for different values of the stellar microturbulence parameter) because the corresponding derived carbon abundance is closer to that of BWO (in which the microturbulence is derived as part of the analysis of the high resolution spectra in the CH region).

To extend our evolutionary sequence to lower luminosity on the giant branch we have obtained new high resolution spectra of two field stars ϕ^2 Ori and ϵ And, whose metallicities are similar to those of the other stars. The new spectra were obtained at the Dominion Astrophysical Observatory with the 1.2-meter telescope, coude spectrograph, long camera and Reticon detector. This combination yields a resolving power of 35,000, and the exposures were timed for a signal-to-noise of about 200. Our spectra cover the C_2 Swan band at 5635 Å, the [O I] line at 6300 Å, the Li line at 6700 Å and the 2-0 red system CN band at 8000 Å, thereby providing abundances of Li, C, N, O as well as iron and the ratio $^{12}\text{C}/^{13}\text{C}$. These stars were analyzed using the same models and gf-values as were used in the other analyses except that the C_2 Swan bands replaced the violet CH bands as the source of the carbon abundance. To analyze the C_2 Swan band at 5635 Å it was necessary to synthesize the spectrum over an interval from 5626-5640 Å. The spectroscopic data for the C_2

Swan bands is that reviewed by Grevesse et al.(1991) in their re-evaluation of the solar C abundance.

Both ϵ And and ϕ^2 Ori have been analyzed by others, most recently with modern model atmospheres and digital spectra by Cottrell & Sneden (1986) and subsequently by SSP93. These two stars provide an overlap with their large sample of stars of generally lower luminosity. We compare their data with ours in Table 2.

Most of the differences between our abundances and those of the Texas group can be understood as due to differences in effective temperatures and gravities. Their lower effective temperatures are responsible for their lower iron abundances and nitrogen abundances because of lower opacities and the dissociation equilibrium of the CN molecule. The low masses derived by SSP93 (Table 6) and of Cottrell & Sneden (1986, Table 6) demonstrate that their gravities are too low by roughly a factor 3 which is the difference between their and our gravity values for the same stars.

Our final adopted abundances are shown in Table 3.

It is important to understand the uncertainties in the individual abundances in Table 3. The iron abundances are almost independent of the CNO abundances but not entirely so. Since many lines of Fe I and several lines of Fe II are easily observed the measured line strengths are not an important source of error. The uncertainty is surely dominated by the uncertainty in the atmospheric model, especially at small optical depth where mechanical energy input and backwarming, such as electron conduction from the chromosphere, can effect the temperature near the boundary, especially the temperature minimum (Kurucz 1996). Hence, we are dealing with an uncertain function, $T(\tau)$, not just an uncertain parameter. This problem

was evaluated carefully by Leep et al.(1987) in connection with the metallicity of M71 and the derivation of solar f -values using either the Holweger-Müller (1974) model or the Bell et al.(1976) model. The conclusion of that paper was that no $[\text{Fe}/\text{H}]$ value for a red giant can be more accurate than ± 0.2 and we accept that here. The influence of CNO abundances on the $[\text{Fe}/\text{H}]$ value comes in through the opacity of CO and CN which effects the atmospheric models. The infrared CO bands are important for the cooling and structure of the outermost layers of an atmosphere of a late-type star, but this effect is less important for stars as warm as those in this study. The CN lines can contribute substantially to the atmosphere structure of red giants because the CN red system blankets a rather large wavelength range near the flux peak, but CN diminishes in importance quickly as the metallicity of a star is decreased because the CN column density falls approximately as metallicity squared while the continuous opacity falls approximately as metallicity.

The uncertainty in the oxygen abundance is mostly determined by the actual measurement of the equivalent width of the only useful oxygen line, $\lambda 6300$, in the globular cluster stars, and the second line at $\lambda 6363$ which is barely detectable in the bright field stars. Since the oxygen line is formed over a wide range of optical depth the derived abundance is not very sensitive to the boundary temperature. The low carbon abundances in these stars means that the uncertainty in the C abundance has little effect on the solution for the O abundance despite the formation of CO in the atmosphere. For oxygen the uncertainties in O/Fe are surely ± 0.1 dex or perhaps a little lower for Arcturus, for which the measurements are by far the most accurate. Hence, the somewhat higher O/Fe value for Arcturus, as compared with the other stars in Table 3, is probably real.

The formation of CO depletes carbon and an error of 0.10 dex in oxygen will cause an error of 0.05 dex in the carbon abundance. Fortunately the CH and C_2 lines are not formed at a small optical depth (as they are in the sun) but rather below the levels at which carbon is depleted by CO formation, so the uncertainty in the boundary temperature is not important. Considering both the uncertainty in the oxygen abundance, the actual measurements of CH, and the presence of some saturation in the CH lines, an uncertainty of 0.15 dex is possible for the ^{12}C abundances.

The $^{12}\text{C}/^{13}\text{C}$ ratio is determined largely by the clump of ^{13}CN lines near 8005 Å. This was illustrated in Figure 3 of BWO: for that star, M13 I-48, a ratio of 6 was derived and the figure shows that a range from 5 to 8 is possible. Scaling that evaluation to Table 2 of this paper indicates that an observed ratio of 7 for three stars could lie between about 5.5 and 9; the pure equilibrium ratio of 3.5-4.0 is pretty well excluded as are values of 10 or above.

The nitrogen abundance, derived from CN lines, is less dependent on line measurement uncertainties because many (~ 15 -20) lines are available in our spectra. However, it does depend on the abundances of C and O through the

dissociation equilibrium of CO, CH, and CN, as well as the formation of N_2 . Hence the uncertainties in the C and O abundances come into play as well as the uncertainty in the CN dissociation potential. For CN the difference between the theoretical value, 7.65 eV (Bauschlicher et al.1988) and the recent experimental value of $7.77 \pm .05$ eV (Costes et al.1990) is disturbing. We have used the 7.65 eV value. If the 7.77 eV value is correct our N abundances must be lowered by 0.2 dex, which lowers our C+N values by a somewhat smaller amount. The reduction in C+N+O introduced by such a reduction in N is .05 dex for Arcturus and the γ Leo pair, and .08 dex for the 47 Tuc stars.

An error in either the dissociation potential of CN or the f -value of the CN red system 2-0 band would effect all of our nitrogen abundances equally. Both of these quantities are not as well determined as might be hoped: the dissociation energy of CN seems to be uncertain by about 0.2 eV, and different sources for the f -values disagree by as much as 30(see the discussion in Bauschlicher et al.1988). The values used here for these quantities, 7.65 eV for D_0^0 and 8.4×10^{-4} for f_{20} , are those used in (for D_0^0) or derived from (f_{20}) the analysis of CN red system lines in the solar spectrum by Sneden & Lambert (1982), so by construction they yield the solar nitrogen abundance. A second source of uncertainty in the N abundance is introduced by the uncertainty in the C abundance. For measured CN lines any error in the C abundance introduces an error of comparable size and opposite sign in the N abundance. Since an error of as much as 0.15 dex in C is possible, an error of the same size with reversed sign is possible for N.

The $^{12}\text{C}/^{13}\text{C}$ ratio also has some observational uncertainty, almost exclusively due to the difference in strength between the ^{12}CN and ^{13}CN lines, so that the microturbulent velocity enters into the isotope ratio solution. This uncertainty is aggravated as the ^{12}CN lines get stronger and as the isotope ratio increases. For the stars in this sample, the ^{12}CN lines are quite weak: for γ Leo A, which has the strongest CN lines in the sample, the reduced equivalent widths are in the range $-5.5 < \log(W/\lambda) < -5.1$, indicating that saturation (and hence microturbulence-related errors in the isotope ratio) are minimal. Our results are summarized in Figures 1 and 3, and discussed below.

3. The onset of extra-mixing on the observed evolutionary sequence

Our observational results are summarized by referring to Figures 1 to 3. We show in Figure 1 the observed dependence of $^{12}\text{C}/^{13}\text{C}$ ratio on M_{bol} . This sequence for our sample of stars with moderate metal deficiencies reveals a behavior of the surface $^{12}\text{C}/^{13}\text{C}$ ratio very similar to the one previously observed at solar metallicity in M67. Three main features appear: (i) The least luminous star, ϕ^2 Ori, shows a depletion of Li by 2.7 dex below the level accepted for young stars and a limit on the $^{12}\text{C}/^{13}\text{C}$ ratio

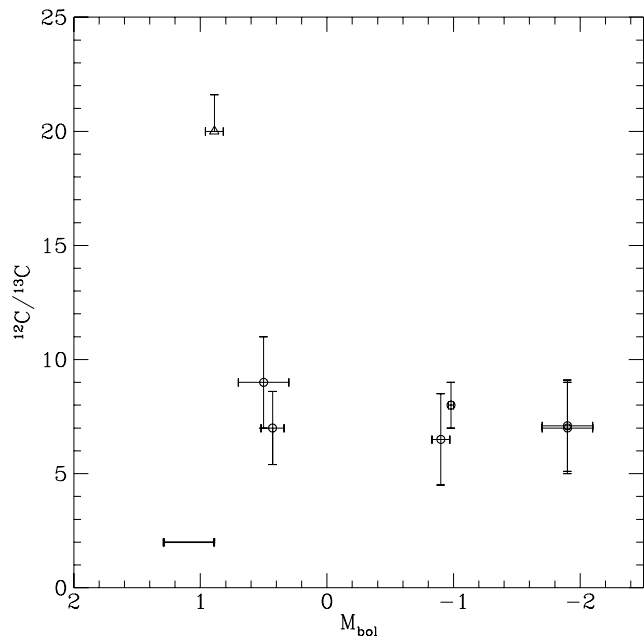


Fig. 1. The ratio of $^{12}\text{C}/^{13}\text{C}$ is plotted against the bolometric magnitude of the program stars. Uncertainties of ± 2 for the isotope ratios are estimated for each star except for Arcturus, for which ± 1 is estimated. The absolute magnitudes are derived from the HIPPARCOS parallaxes. Note that 47 Tuc 3501 and 4418 have both the same luminosity and carbon isotopic ratio. The horizontal line indicates the position of the bump in the luminosity function of 47 Tuc (King et al.1985).

in agreement with standard predictions for dilution ² This indicates that the standard theoretical main sequence profiles of ^{12}C and ^{13}C match the real chemical profiles, and that the extra-mixing is only efficient after the completion of the first dredge-up (see C94). (ii) Then between $M_{\text{bol}} = +0.9$ and $+0.5$, the observed isotopic ratio drops to values near 7, well below the standard predicted post-dilution ratio. It is interesting to note that in the RGB luminosity function of 47 Tuc, King, et al.(1985) localize the bump at $M_{\text{bol}} = +1.05 \pm 0.2$, i.e. precisely in the region where the disagreement between standard predictions and observations of the carbon isotopic ratio appears in our sample. This confirms that the extra-mixing which leads to very low $^{12}\text{C}/^{13}\text{C}$ ratios in low-mass and metal-deficient evolved stars becomes efficient exactly when the hydrogen-burning shell crosses the chemical discontinuity created by the outward moving convective envelope. (iii)

² (All the standard models computed by different authors give very similar result for the post-dredge up value of $^{12}\text{C}/^{13}\text{C}$; see for example the compilation by Wasserburg et al. 1995. Boothroyd & Sackman (1997) showed that different initial carbon isotopic ratio do not affect significantly the post-dredge up result, whatever the metallicity of the models.)

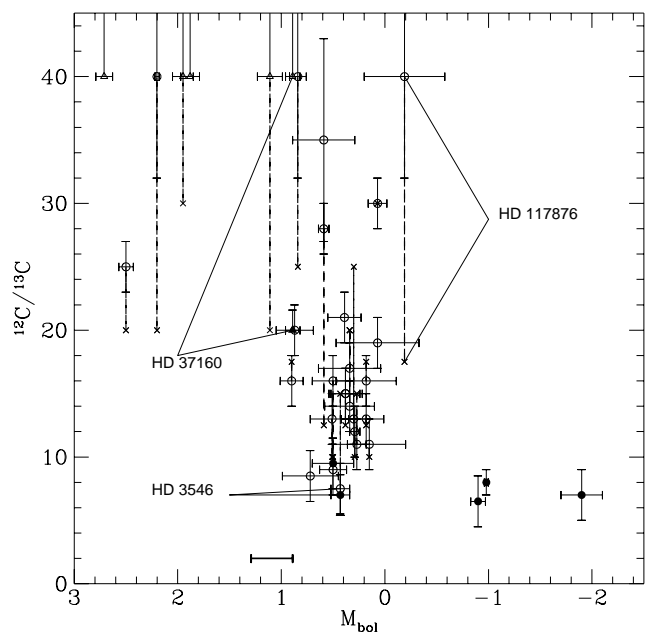


Fig. 2. Carbon isotopic ratios for the old disk giants by Cottrell & Sneden (1986; crosses) and Shetrone et al.(1993; open circles and triangles). Our program stars are also shown (black circles and triangle). Observations for the same stars are connected by broken lines. The absolute magnitudes are derived from the HIPPARCOS parallaxes. The horizontal line indicates the position of the bump in the luminosity function of 47 Tuc (King et al.1985).

Finally, from $M_{\text{bol}} = +0.4$ to -2 , there is no further change in the $^{12}\text{C}/^{13}\text{C}$ ratio.

The “abrupt” change in $^{12}\text{C}/^{13}\text{C}$ ratio shortly after the luminosity-function bump occurs both at solar and at lower metallicities, although the final $^{12}\text{C}/^{13}\text{C}$ ratio is lower in the more metal-poor stars. It is worth noting that the change in $^{12}\text{C}/^{13}\text{C}$ ratio is “abrupt” only in terms of stellar luminosity. The LFB is caused by a slower rate of evolution for stars at this luminosity (that is, dL/dt is smaller there) owing to the H-burning shell contacting the H-rich, previously mixed, zone; of the time stars take to evolve from the beginning of the LFB to the tip of the giant branch, 15 — 20% of it is spent in the LFB. Consequently, the change in the $^{12}\text{C}/^{13}\text{C}$ ratio may not be so abrupt in terms of time.

In order to enlarge our sample, we recomputed the absolute magnitudes from the HIPPARCOS parallaxes for the old disk giants with $^{12}\text{C}/^{13}\text{C}$ ratios derived by SSP93. These stars also have moderate metal deficiencies ($-1.0 \leq [\text{Fe}/\text{H}] \leq -0.3$). Due to the good luminosity determination, the complete data, which are presented in Figure 2, can be reasonably viewed as an evolutionary sequence. We also show the $^{12}\text{C}/^{13}\text{C}$ ratios previously derived by

Cottrell & Sneden (1986) for the stars which belong to the SSP93 sample.

The SSP93 isotope ratios tend to be systematically higher than the Cottrell & Sneden values for stars with high $^{12}\text{C}/^{13}\text{C}$, but this is easily understood as being due to SSP93's superior spectral resolution. The higher spectral resolution allows detection and better measurement of the very weak ^{13}CN features. This highlights a general problem in the determination of $^{12}\text{C}/^{13}\text{C}$ ratios: three effects operate to make ^{13}CN detection difficult for low-luminosity stars. First, at lower luminosities the ^{13}CN proportion is lower due to their unmixed state. Second, model atmosphere effects operate so that higher-gravity, lower-luminosity stars have weaker CN lines even for constant chemical composition in the atmosphere. Third, the lower stellar luminosity makes it more difficult to obtain the requisite S/N to detect the weak lines.

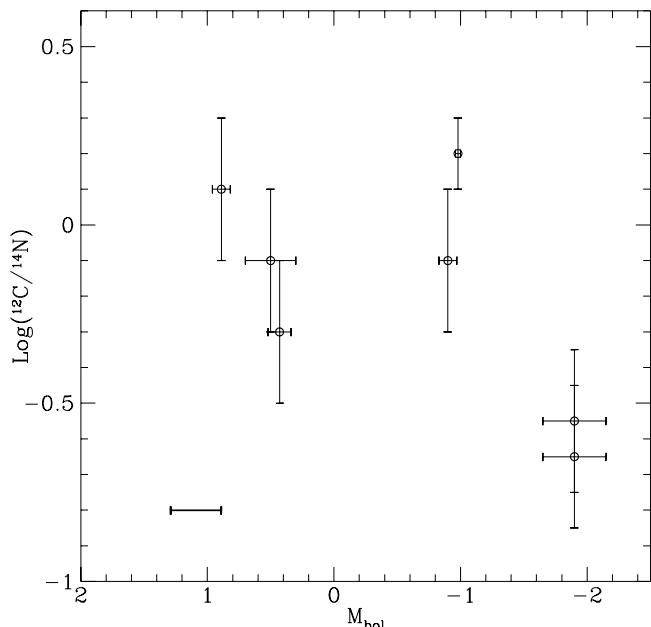


Fig. 3. $\text{Log } ^{12}\text{C}/^{14}\text{N}$ against M_{bol} for the program stars. The uncertainty in $\text{log } ^{12}\text{C}/^{14}\text{N}$ is estimated to be 0.2 dex except for Arcturus, for which it is probably 0.1 dex. The horizontal line indicates the position of the bump in the luminosity function of 47 Tuc (King et al.1985).

Despite the uncertainties, it is clear that in the present complete sample, no star with $M_{\text{bol}} > +1.0$ shows a carbon isotopic ratio lower than the one predicted by standard dilution models. Figure 2 is strong evidence that extra mixing begins at a luminosity of about $M_{\text{bol}} = +1$. This limit in luminosity corresponds to the approximative value for $M_{\text{bol}}(\text{bump})$ observed in clusters of the same $[\text{Fe}/\text{H}]$ as the present stars (Fusi Pecci et al.1990). The

cutoff region appears broader here than in our restricted sample, mainly due to a probable scatter in the stellar masses in SSP93 data. Indeed, a $0.1M_{\odot}$ difference corresponds approximatively to a shift of 0.2 in M_{bol} for the position of the bump (Fusi Pecci et al.1990).

We show the observed $^{12}\text{C}/^{14}\text{N}$ ratios plotted against M_{bol} in Figure 3. ϕ^2 Ori presents a ratio consistent with standard post-dredge-up predictions. The $^{12}\text{C}/^{14}\text{N}$ ratio decreases simultaneously with the $^{12}\text{C}/^{13}\text{C}$ ratio between $M_{\text{bol}} = +1.0$ and $+0.5$ by about 0.3 dex, revealing that the extra-mixing process also slightly affects the N abundance. Arcturus, for which the data is by far the best due to its brightness, stands however above the curve for the other stars (which really means above γ Leo A, at the same luminosity, by 0.3 dex).³ This difference was recognized easily 15 years ago by Lambert & Ries (1981), who found a difference of 0.47 dex. The 47 Tuc stars, at $M_{\text{bol}} = -1.9$, present $^{12}\text{C}/^{14}\text{N}$ ratios lower than those in the less evolved objects.

In the M67 data (Brown 1987), a change in the C/N ratio at and above the luminosity of the RGB bump is not clear. This is probably due to errors, both random and systematic, in the abundances derived from the synthetic spectrum fits, and aggravated by the sparseness of the cluster RGB. A systematic offset in the nitrogen abundance was found in that study, and an attempt was made to calibrate this out in a post hoc way. The result, however, is that any slow trend in C/N with luminosity in the Brown (1987) data must be interpreted with caution. It is more secure, however, to note that the total change in the C/N ratio between stars at the base of the giant branch and those at the RGB tip and in the post-helium core flash clump is larger than predicted in standard models, so that the most luminous M67 giants again have also engaged in some extra mixing.

In our sample, the Li abundance drops between ϕ^2 Ori and ε And (in terms of luminosity) after which it is below detectability. It is difficult however to argue for the luminosity onset of extra-mixing from this data. Indeed, lithium destruction on the main sequence may lead to a dispersion of the abundances on the red giant branch which could explain the difference between ϕ^2 Ori and ε And. In any case, the lithium abundances in the more evolved stars from our sample clearly indicates that an extra-mixing mechanism transports lithium from the convective envelope down to the region where it is destroyed by proton capture after the end of the dilution phase. In a large sample of evolved halo stars, Pilachowski, Sneden & Booth (1993) also showed that the lithium abundance continues to decrease after the completion of the first dredge-up.

³ Aoki and Tsuji (1997) have reanalysed the N abundance in Arcturus (and many cooler stars) and find $\text{log}(^{12}\text{C}/^{14}\text{N}) = 0.09$, which is within our uncertainty and somewhat closer to the $^{12}\text{C}/^{14}\text{N}$ ratio in Gamma Leo A.

4. Determination of a critical μ -gradient from the observed carbon isotopic ratios

Recently, different groups have simulated extra-mixing between the base of the convective envelope and the hydrogen burning shell in order to reproduce the CNO abundances in RGB stars. Denissenkov & Weiss (1995) modeled this deep mixing by adjusting both the mixing depth and rate in their diffusion procedure. Wasserburg et al. (1995) and Boothroyd & Sackman (1997) used an ad-hoc “conveyor-belt” circulation model, where the depth of the extra-mixed region is related to a parametrized temperature difference up to the bottom of the hydrogen-burning shell. On the other hand, other authors attempted to relate the extra-mixing with physical processes, among which rotation seems to be the most promising. Sweigart & Mengel (1979) suggested that meridional circulation on the RGB could lead to the low $^{12}\text{C}/^{13}\text{C}$ observed in field giants. Taking into account the interaction between meridional circulation and turbulence induced by rotation in stars, Charbonnel (1995) showed that rotation-induced mixing can account for the observed behavior of carbon isotopic ratios and for the Li abundances in Population II low mass giants.

In these different approaches, the common underlying question is the determination of the extension of the region where extra-mixing occurs, and more precisely the nature of the stabilizing factor. An investigation into the mechanism of extra mixing must include an understanding of why the mechanism does *not* operate at luminosities below that of the RGB bump, and what is the nature of the factor that stabilizes the star against extra mixing before it reaches this point. When suggesting that the extra-mixing on the RGB could be related to rotation, Sweigart & Mengel (1979) and Charbonnel (1994, 1995) underlined the inhibiting effect of molecular weight (or μ) barriers. Indeed, as argued by Mestel (1957), gradients of molecular weight tend to restrain the circulation and to stabilize the mixing processes related to rotation. We will show now how the observations gathered in this paper allow us to constrain, from simple considerations, the conditions in which a μ -barrier shields the central regions of a star from extra-mixing.

We have computed some standard stellar models for exploration of these questions. The evolutionary sequences were followed from the pre-main sequence up to the RGB tip with the Toulouse-Geneva code (see Charbonnel et al. 1992). The input microphysics is the same as used in Charbonnel et al. (1997). The relative ratios for the heavy elements correspond to the mixture by Grevesse & Noels (1993). We take the same isotopic ratios as Maeder (1983). Neither element segregation or rotation-induced mixing are included in the present computations.

The gradients of molecular weight ($\nabla \ln \mu = d \ln \mu / dr$) in a standard stellar model of $0.9M_{\odot}$ with $[\text{Fe}/\text{H}] = -0.45$, typical of the present observed sample, are presented in

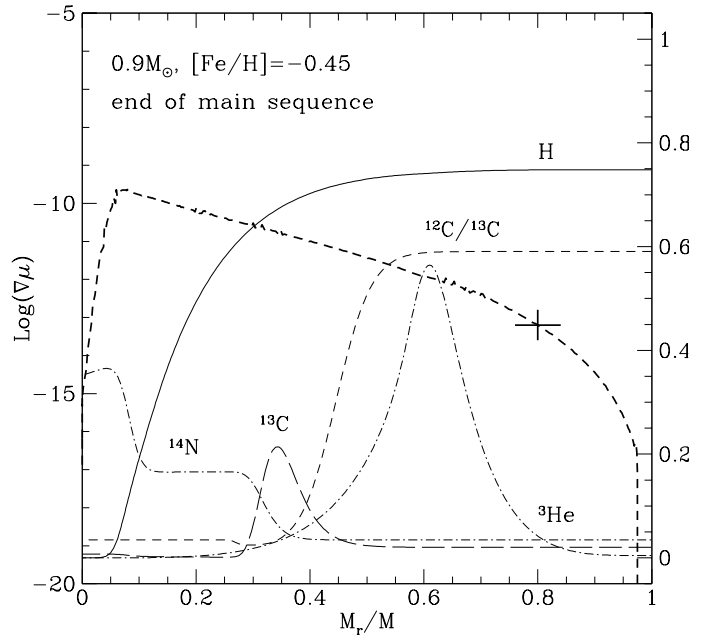


Fig. 4. Molecular weight gradient (in log scale, bold dashed line, left axis) and composition profiles (right axis) in a $0.9M_{\odot}$, $[\text{Fe}/\text{H}]=-0.45$ stellar model, at the end of the main sequence. The mass fractions are multiplied by 100 for ^3He and ^{14}N , by 1000 for ^{13}C ; the ratio $^{12}\text{C}/^{13}\text{C}$ is divided by 100. The thick cross corresponds to $(\nabla \ln \mu)_c$, the critical molecular weight gradient obtained with the prescription by Huppert & Spiegel (1977) discussed in §5

Figures 4, 5 and 6 at three different evolutionary stages: at the end of the main sequence, after the completion of the first dredge-up, and shortly after the RGB bump. We also show the abundance profiles for H, ^3He , ^{13}C and ^{14}N , and the $^{12}\text{C}/^{13}\text{C}$ ratio.

While on the main sequence, nuclear burning leads to an increase of the mean molecular weight in the central regions of the star (see Figure 4). During the first dredge-up phase, the convective envelope homogenizes the star down to very deep regions, and builds a very steep gradient of molecular weight at the point of its maximum penetration ($\nabla \ln \mu \simeq 10^{-6}$ at $M_r/M \simeq 0.282$ in Figure 5). Further on, as the star keeps ascending the RGB, the hydrogen burning shell becomes thinner and moves outwards in the mass scale, while the convective envelope retreats. As discussed in §3, our observations provide strong evidence that the extra-mixing is inhibited until the star reaches the LFB. The shape of $\nabla \ln \mu$ just after this evolutionary point, i.e. after the encounter of the hydrogen burning shell with the previously mixed region, is shown in Figure 6. Below the base of the convective envelope $\nabla \ln \mu$ is much lower at this time.

Our observations provide a precise clue on the extension of the extra-mixed region down to the nuclear burning

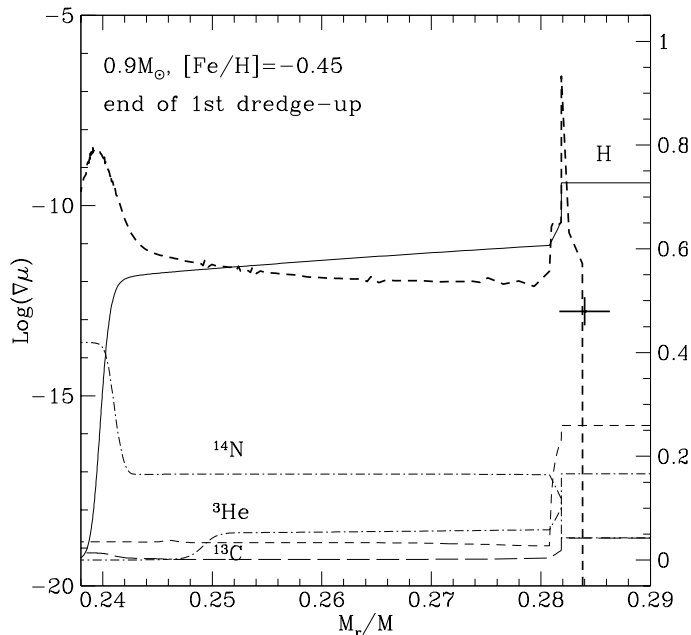


Fig. 5. Same as Fig. 4, after the completion of the first dredge-up, in the H-burning shell region. The base of the convection zone is located at $M_r/M \simeq 0.283$.

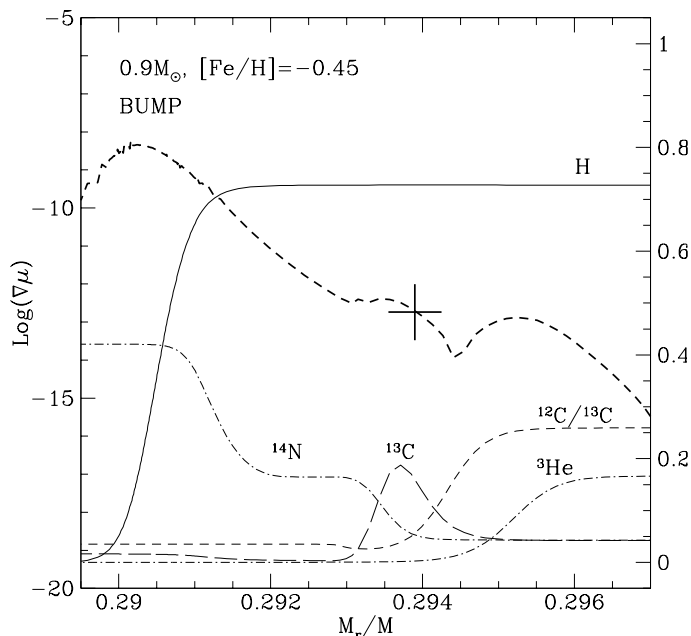


Fig. 6. Same as Fig. 4, after the RGB bump, in the H-burning shell region. The base of the convection zone is located at $M_r/M \simeq 0.313$.

layers. The low $^{12}\text{C}/^{13}\text{C}$ ratios we see in our sample ($\simeq 7$) can indeed be reached if the extra-mixing develops down to $M_r/M \simeq 0.294$ in our $0.9M_{\odot}$ model (see Figure 6). At this point, $\nabla \ln \mu \simeq 1.5 \times 10^{-13}$. We now assign this value to $(\nabla \ln \mu)_{c,obs}$, that we define as the “observational” critical μ -gradient which appears to shield the central regions of the star from extra-mixing. In our $0.9M_{\odot}$ model, the temperature difference $\Delta \log T$ between the bottom of the hydrogen burning shell and this point is equal to 0.26. This value for $\Delta \log T$ is in agreement with the one Boothroyd & Sackman (1997) have to impose in their parametrized mixing model in order to match the observed $^{12}\text{C}/^{13}\text{C}$ ratios at solar metallicity.

Let us check now to what region $(\nabla \ln \mu)_{c,obs} \simeq 1.5 \times 10^{-13}$ corresponds, in terms of expected $^{12}\text{C}/^{13}\text{C}$, at different evolutionary stages, and for stars of different metallicities. We see in Figure 4 that while the star is on the main sequence, the real $\nabla \ln \mu$ becomes higher than $(\nabla \ln \mu)_{c,obs}$ in the very external part of the star, around M_r/M equal to 0.75. If we assume that such a μ -barrier can not be penetrated, then on the main sequence no extra-mixing is expected to occur in the stellar region of energy production. This explains the observations of the carbon isotopic ratio in ϕ^2 Ori, in the less luminous stars of SSP93’s sample, and in the less evolved RGB stars of M67 (GB91), where we see a perfect agreement with standard theoretical dilution. This is also in agreement with helioseismological constraints. Indeed, solar structure computations bring important information on the critical μ -gradients that limit the mild mixing which is necessary to explain the lithium depletion in the Sun. Richard et al. (1996) and Richard & Vauclair (1997) showed that the best solar models (for what concerns helioseismological comparison and agreement with Li and Be observations) are those including both element segregation and rotation-induced mixing, where the mixing is cut-off when the μ -gradient becomes \geq to $1.5 - 4 \times 10^{-13}$. It is highly satisfactory to get the same value for $(\nabla \ln \mu)_{c,obs}$ from two completely different observational constraints.

The gradients of molecular weight shortly after the RGB bump in a model of $0.9M_{\odot}$ with $[\text{Fe}/\text{H}] = -2$ (typical of a globular cluster giant) and in a model of $1.25M_{\odot}$ at solar metallicity (typical of a M67 giant star) are presented respectively in Figures 7 and 8. If we assume that the extra-mixing reaches down to the same $(\nabla \ln \mu)_{c,obs}$ whatever the star, then the $^{12}\text{C}/^{13}\text{C}$ is expected to decrease down to its equilibrium value for the globular cluster giant, and down to $\simeq 12$ in the open cluster giant. These values, and the dependency with metallicity, are exactly as observed in the giants in open clusters by Gilroy (1989) and are in agreement with the other observations of field stars and globular cluster giants. They are independent of any modeling for the extra-mixing. It appears then that the value we derived empirically for $(\nabla \ln \mu)_{c,obs}$ is “universal”, in the sense that an unique value is sufficient to describe different constraints.

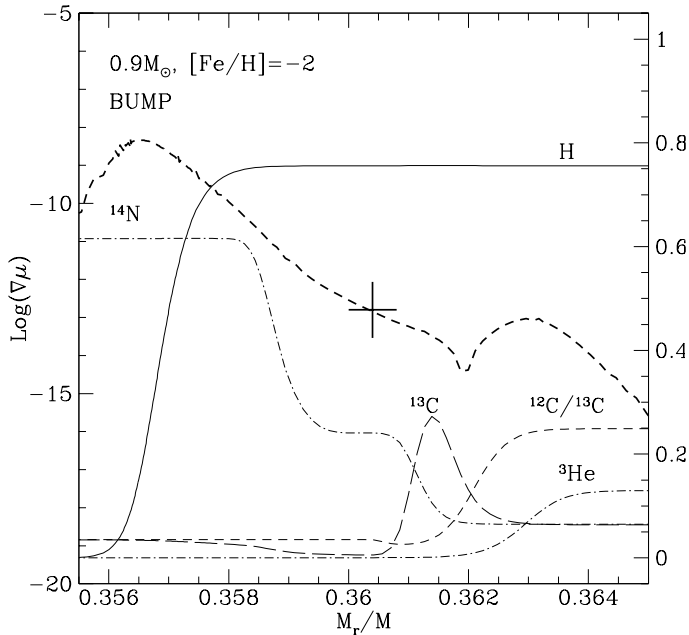


Fig. 7. Same as Fig. 6 in the $0.9M_{\odot}$, $[\text{Fe}/\text{H}]=-2$ stellar model. The base of the convection zone is located at $M_r/M \approx 0.387$. The mass fractions are multiplied by 100 for ${}^3\text{He}$, and by 50000 and 5000 respectively for ${}^{13}\text{C}$ and ${}^{14}\text{N}$; the ratio ${}^{12}\text{C}/{}^{13}\text{C}$ is divided by 100

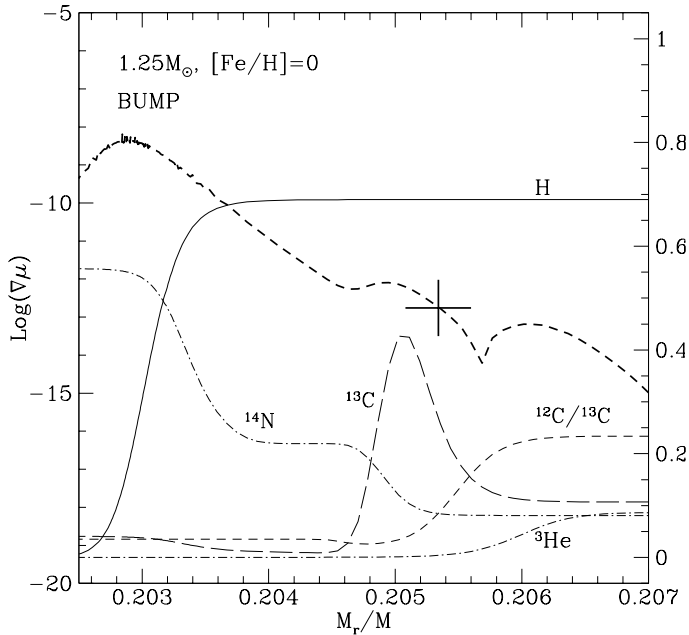


Fig. 8. Same as Fig. 6 in the $1.25M_{\odot}$, $[\text{Fe}/\text{H}]=0$ stellar model. The base of the convection zone is located at $M_r/M \approx 0.218$. The mass fractions are multiplied by 100, 1000 and 50 respectively for ${}^3\text{He}$, ${}^{13}\text{C}$ and ${}^{14}\text{N}$; the ratio ${}^{12}\text{C}/{}^{13}\text{C}$ is divided by 100

As already shown by C94, if molecular weight barriers are the inhibiting factor, then no extra-mixing is expected to occur in stars which ignite helium in a non-degenerate core, i.e. in stars with masses higher than 1.7 to $2.2M_{\odot}$ (the exact value depends on the metallicity). Indeed, in these more massive stars, the hydrogen burning shell does not have the time to reach the regions that have been homogenized during the first dredge-up, so that $(\nabla \ln \mu)$ below the convective envelope is always higher than $(\nabla \ln \mu)_{c,obs}$. Under these conditions, extra-mixing is inhibited in these stars. This is confirmed by the observational data in open clusters with turn-off masses higher than about $2M_{\odot}$ (Gilroy 1989).

5. Clues on the nature of the extra-mixing process on the rgb

The results described previously were obtained using observational constraints only, and did not rely on any special prescription for the extra-mixing. We can nevertheless check whether the value we get for $(\nabla \ln \mu)_{c,obs}$ is consistent with what is expected in a very simplified rotation framework. Let us follow the suggestion by Huppert & Spiegel (1977) according to which meridional currents can penetrate into a region with a stable gradient of molecular weight within a scale height given by $h \simeq r \frac{\Omega(r)}{N_{\mu}}$, where r is the local radius, $\Omega(r)$ is the angular rotation velocity, and N_{μ} the buoyancy frequency due to the μ -gradients. We can derive then a critical μ -gradient by specifying that h must be a small fraction of r ($h = \epsilon r$): $(\nabla \ln \mu)_{c,theor} \simeq \frac{1}{\epsilon^2} \frac{r^2 \Omega^2(R_c)}{GM(r_c)}$, where all the quantities are computed at the place where the actual $\nabla \ln \mu$ is equal to the critical one.

For each of our 3 models, we computed $(\nabla \ln \mu)_{c,theor}$ for a stellar rotation velocity of 2.5 km sec^{-1} , typical on the RGB for the stellar masses in consideration (De Medeiros et al. 1996). The $(\nabla \ln \mu)_{c,theor}$ we obtain in this model-dependent approach are shown in Figures 4 to 8 (thick cross). They are in perfect agreement with the constraints coming from the observations discussed in §4. This result tends to indicate that the extra-mixing process on the RGB is related to rotation.

However, we have to be cautious in our conclusions. Indeed, $(\nabla \ln \mu)_{c,theor}$ is derived here in a simplified framework. Complete computations with rotation-induced mixing have to be performed. The transport of chemicals and angular momentum should be treated simultaneously to properly handle the development of μ -barriers (despite rotational mixing) during stellar evolution. Different stellar rotational histories also have to be considered, which may result in different efficiencies of the extra-mixing, and lead to a dispersion of chemical anomalies from star to star. Observational support for this approach may exist from the variations of oxygen abundances and rotational ve-

locities in blue horizontal branch stars in three globular clusters (Peterson et al.1995).

6. Conclusions

We have assembled accurate $^{12}\text{C}/^{13}\text{C}$ ratios, as well as abundance data for C, N, O and Li for five field giants with $[\text{Fe}/\text{H}] \simeq -0.5$ including Arcturus, and for two stars in the globular cluster 47 Tuc, and reviewed previously published data for a number of other field giants. Using HIPPARCOS parallaxes to derive M_{bol} values, we placed these stars into an evolutionary sequence along the ascent of the RGB. The sequence shows that the $^{12}\text{C}/^{13}\text{C}$ ratios drops from ~ 20 to near 7 between $M_{\text{bol}} = +0.9$ and $+0.5$, while Li disappears. The C/N ratio is also affected, with $\log(^{12}\text{C}/^{14}\text{N})$ diminishing from $+0.1$ to -0.6 between $M_{\text{bol}} = +0.9$ and -2 . Arcturus stands above the curve defined by the other stars by 0.4 dex. These observations confirm the existence of an extra-mixing process that becomes efficient on the RGB only when low-mass stars reach the so-called luminosity-function bump. This result is established for the first time for stars with moderate metal deficiencies.

We used the values of the carbon isotopic ratio observed in our sample to get constraints on the μ -barriers that may shield the central regions of a star from extra-mixing. We showed that the same value of the critical gradient of molecular weight leads to $^{12}\text{C}/^{13}\text{C}$ ratios observed at different metallicities. This observational critical μ -gradient is in very good agreement with the critical μ -gradient which is expected to stabilize meridional circulation. This result brings strong clues on the nature of the extra-mixing which occurs on the RGB, and indicates that it is related to rotation. Observational support for this approach may exist from the variations of oxygen, sodium and aluminum in globular cluster red giants as well as the measurement of rotational velocities in blue horizontal branch stars in three globular clusters (Kraft, 1994; Kraft et al., 1997; Peterson et al. 1995).

We thank the Institute for Nuclear Theory at the University of Washington where this work was initiated. C.C. is most appreciative for the hospitality shown to her while a visitor at the Space Telescope Science Institute. G.W. and J.A.B. would like to acknowledge the support of the Kennilworth Fund of the New York Community Trust. Some of the spectra were obtained by Guillermo Gonzalez. The spectra analyzed as part of this project were obtained at the Dominion Astrophysical Observatory, Herzberg Institute of Astrophysics, National Research Council, Canada.

References

- Anders, E. and Grevesse, N. 1989, *Geochim. Cosmochim. Acta*, 53, 197
- Aoki, W., Tsuji, T., 1997, $\dot{\text{A}}$, in press
- Bauschlicher, C. W., Jr., Langhoff, S. R. and Taylor, P. R. 1988, *ApJ*, 332, 531
- Bell, R. A., Dickens, R. J., & Gustafsson, B. 1979, *ApJ*, 229, 604
- Bell, R. A., Briley, M. M. and Smith, G. H. 1990, *AJ*, 100, 187
- Bell, R. A. Gustafsson, B., Eriksson, K. and Nordlund, 1976, *A&AS*, 23, 37
- Boothroyd, A. and Sackman, I. 1997, preprint
- Briley, M. M., Bell, R. A., Hoban, S., & Dickens, R. J. 1990, *ApJ*, 359, 307
- Briley, M. M., Smith, V. V., and Lambert, D. L. 1994, *ApJ Letters*, 424, L119
- Briley, M. M., Smith, V. V., King, J., & Lambert, D. L. 1997, *AJ*, 113, 306
- Brown, J. A. 1987, *ApJ*, 317, 701
- Brown, J. A. and Wallerstein, G. 1989, *AJ*, 98, 1643
- Brown, J. A. and Wallerstein, G. 1992, *AJ*, 104, 1818
- Brown, J. A., Wallerstein, G. and Oke, J. B. 1990, *AJ*, 100, 1561 (BWO)
- Brown, J. A., Wallerstein, G. and Oke, J. B. 1991, *AJ*, 101, 1693
- Buser, R., & Kurucz, R. L. 1992, *A&A*, 264, 557
- Carbon, D. F., et al.1982, *ApJ Suppl*, 49, 207
- Charbonnel, C., Vauclair, S. & Zahn, J. P. 1992, *A&A*, 255, 191
- Charbonnel, C. 1994, *A&A*, 282, 811 (C94)
- Charbonnel, C. 1995, *ApJ*, 453, L41
- Charbonnel, C., Däppen, W., Bernasconi, P.A., Maeder, A., Schaerer, D., Mowlavi, N., 1997, *A&ASubmitted*
- Costes, M., Naulin, C. and Dorthe, G. 1990, *A&A*, 232, 270
- Cottrell, P. L. and Sneden, C. 1986, *A&A*, 161, 314
- Day, R. W., Lambert, D. L., & Sneden, C. 1973, *ApJ*, 185, 213
- De Medeiros, J. R., Da Rocha, C., & Mayor, M. 1996, *A&A*, 314, 499
- Denissenkov, P. A., and Weiss, A. 1995, *A&A*, 308, 773
- DiBenedetto, G. P. 1993 *A&A*, 270, 315
- Drake, J. J., Smith, V. V., & Suntzeff, N. B. 1992 *ApJ Letters*, 395, L95
- Dyck, H. M., Benson, J. A., van Belle, G. T., & Ridgway, S. T. 1996, *AJ*, 111, 1705
- Fusi Pecci, F., Ferraro, F. R., Crocker, D. A., & Rood, R. T. 1990 *A&A*, 238, 95
- Gilroy, K. K. 1989, *ApJ*, 347, 835
- Gilroy, K. K. and Brown, J. A. 1991, *ApJ*, 371, 578 (GB91)
- Grevesse, N., Noels, A., 1983, in "Origin and Evolution of the Elements", Eds. Prantzos N., Vangioni-Flam E., Cassé M.
- Grevesse, N., Lambert, D. L., Sauval, A. J., van Dishoeck, E. F., Farmer, C. B., & Norton, R. H. 1991, *A&A*, 242, 488
- Helfer, H. L., & Wallerstein, G. 1986, *ApJ Suppl*, 16, 1
- Hesser, J. R., Harris, W. E., VandenBerg, D. A., Allwright, J. W. B., Shott, P. and Stetson, P. B. 1987, *PASP*, 99, 739
- Holweger, H. and Müller, E. A. 1974, *Sol. Phys.*, 39, 19
- Huppert, H. E., and Spiegel, E. A. 1977, *ApJ*, 213, 157
- King, C. R., Da Costa, G. S., and DeMarque, P. 1985 *ApJ*, 299, 674
- Kraft, R. P., Sneden, C., Langer, G. E., & Prosser, C. F. 1992, *AJ*, 104, 645
- Kraft, R. P., Sneden, C., Langer, G. E., & Shetrone, M. D. 1993, *AJ*, 106, 1490
- Kraft, R. P. 1994, *PASP*, 106, 553

- Kraft, R. P., Sneden, C., Smith, G. H., Shetrone, M. D., Langer, G. E., & Pilachowski, C. A. 1997, *AJ*, 113, 279
- Kurucz R.L., 1996, in *Model Atmospheres and Spectrum Synthesis*, eds. S.J. Adelman, F. Kupka, and W.W. Weiss. ASP Conference Series v 108 (San Francisco: ASP) p 2.
- Lambert, D. L., Dominy, J. F., & Sivertsen, S. 1980, *ApJ*, 235, 114
- Lambert, D. L. and Ries, L. M. 1981, *ApJ*, 248, 228
- Langer, G. E., Kraft, R. P., Carbon, D. F., Friel, E., & Oke, J. B. 1986 *PASP*, 98, 473
- Leep, E. M., Oke, J. B. and Wallerstein, G. 1987, *AJ*, 93, 1137
- Maeder A., 1983, *A&A* 120, 113
- Mestel, L. 1957, *ApJ*, 126, 550
- Meynet, G., Mermilliod, J.-C., & Maeder, A. 1993, *A&AS*, 98, 477
- Nissen, P. E., & Høg, E. 1997, in *HIPPARCOS Venice Symposium*, ESA SP-402
- Norris, J. E., and Da Costa, G. S. 1995, *ApJ Letters*, 441, L81
- Paltoglou, G., and Norris, J. E. 1989, *ApJ*, 336, 185
- Peterson, R. C., Rood, R. T., & Crocker, D. A. 1995, *ApJ*, 453, 214
- Pilachowski, C. A. 1988, *ApJ Letters*, 326, L57
- Pilachowski, C. A., Sneden, C., and Booth, J. 1993, *ApJ*, 407, 699
- Richard, O., Vauclair, S., Charbonnel, C., & Dziembowski, W. A. 1996, *A&A*, 312, 1000
- Richard, O., & Vauclair, S. 1997, *A&A*, 322, 671
- Ridgway, S. T., Joyce, R. R., White, N. M., & Wing, R. F. 1980, *ApJ*, 235, 126
- Reid, I. N. 1997, *AJ*, 114, 161
- Ries, L. M. 1991, PhD thesis, University of Texas
- Shetrone, M. D., Sneden, C. and Pilachowski, C. A. 1993, *PASP*, 105, 337 (SSP93)
- Shetrone, M. D. 1996, *AJ*, 112, 2639
- Smith, V. V., and Suntzeff, N. B. 1989, *AJ*, 97, 1699
- Sneden, C., & Lambert, D. L, 1982, *ApJ*, 259, 381
- Sneden, C., Pilachowski, C. A. and VandenBerg, D. A. 1986, *ApJ*, 311, 826
- Sneden, C., Kraft, R. P., Prosser, C. F., & Langer, G. E. 1991, *AJ*, 102, 2001
- Suntzeff, N. B. 1981, *ApJ Suppl*, 47, 1
- Suntzeff, N. B., and Smith, V. V. 1991, *ApJ*, 381, 160
- Sweigart, A. V., and Mengel, J. G. 1979, *ApJ*, 229, 624
- Trefzger, C. F., Carbon, D. F., Langer, G. E., Suntzeff, N. B., and Kraft, R. P. 1983, *ApJ*, 266, 144
- Trimble, V. and Bell, R. A. 1981, *DJRAS*, 22, 361
- VandenBerg, D. A. 1985, *ApJ Suppl*, 58, 711
- Wasserburg, G. J., Boothroyd, A. I., and Sackman, I.-J. 1995, *ApJ*, 447, L37
- Zucker, D., Wallerstein, G., & Brown, J. A. 1996, *PASP*, 108, 911